高精度位置天文解析手法の開発とシミュレーションによる検証

大澤亮
JASMINE project, National Astronomical Observatory of Japan

河田大介 (UCL), 上塚貴史 (東京大学), 山田良透 (京都大学),
Wolfgang Löffler, Michael Biermann (ARI/ZAH), JASMINE データ解析チーム

Overview

We developed the Plate Analysis algorithm for wide-area & relative astrometry.

The algorithm is built on the following assumptions.

- The apparent motions of sources are negligible within a dataset.
- The image distortion pattern is consistent within a dataset.

We developed software to obtain astrometric solutions for the Plate Analysis.

- The observation model is implemented with JAX and differentiable.
- Parameters are optimized with SVI, accelerated with JAX & numpyro.

The software successfuly provided a reasonable solution in a validation test.

Table of Contents

Power of Astrometry

Astrometry = Strong tool to reveal the history of the Milky Way (galactic archaeology, GA)

Gaia measures proper motions and parallaxes at ~10 μas/yr & 10 μas levels.

Several relics of satellite merges are discovered.

The Gaia-Sausage-Enceladus in the inner halo

The remnant of a major merger that formed the inner halo possibly occurred about 100 Gyr ago

The phase spiral of the Galactic disk

The after effect of a satellite galaxy passage about 10 Gyr ago, which disturbed the Galactic disk in a phase space

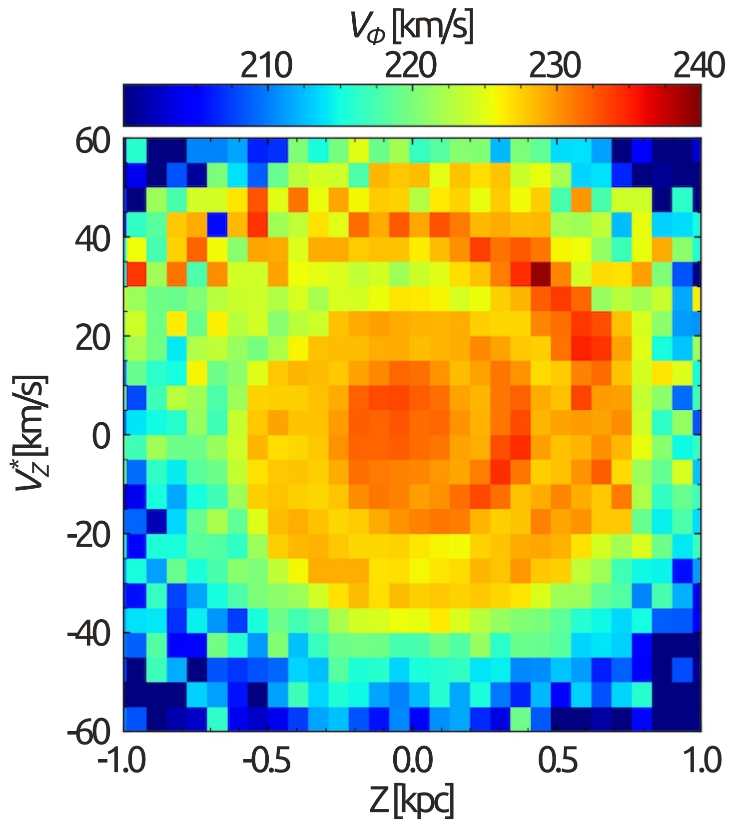

e.g., Belokurov et al. (2018), Antoja et al. (2023), Antoja et al. (2018)

Astrometric Frontier

Galactic center regions is not inspected by *Gaia*.

Sources at > 4 kpc are heavily obscured by interstellar dust.

Formation of the bar, bulge, and NSD can be inspected by the Galactic center astrometry.

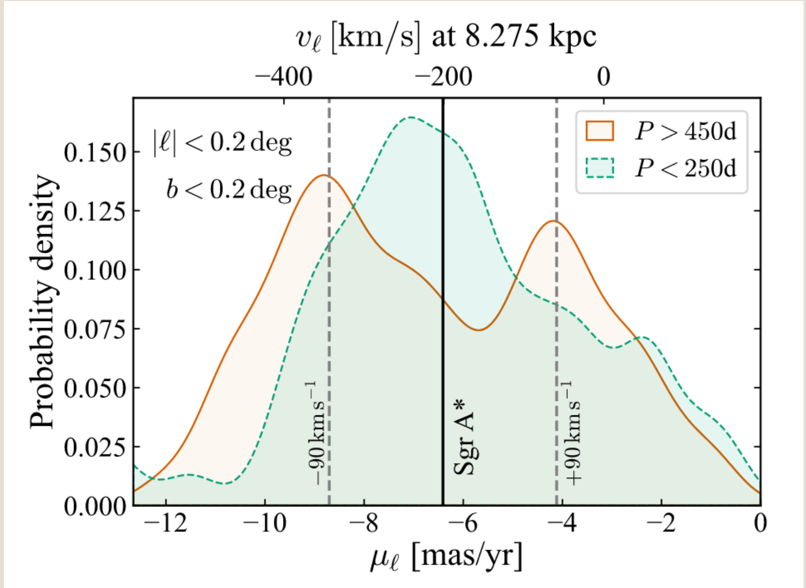

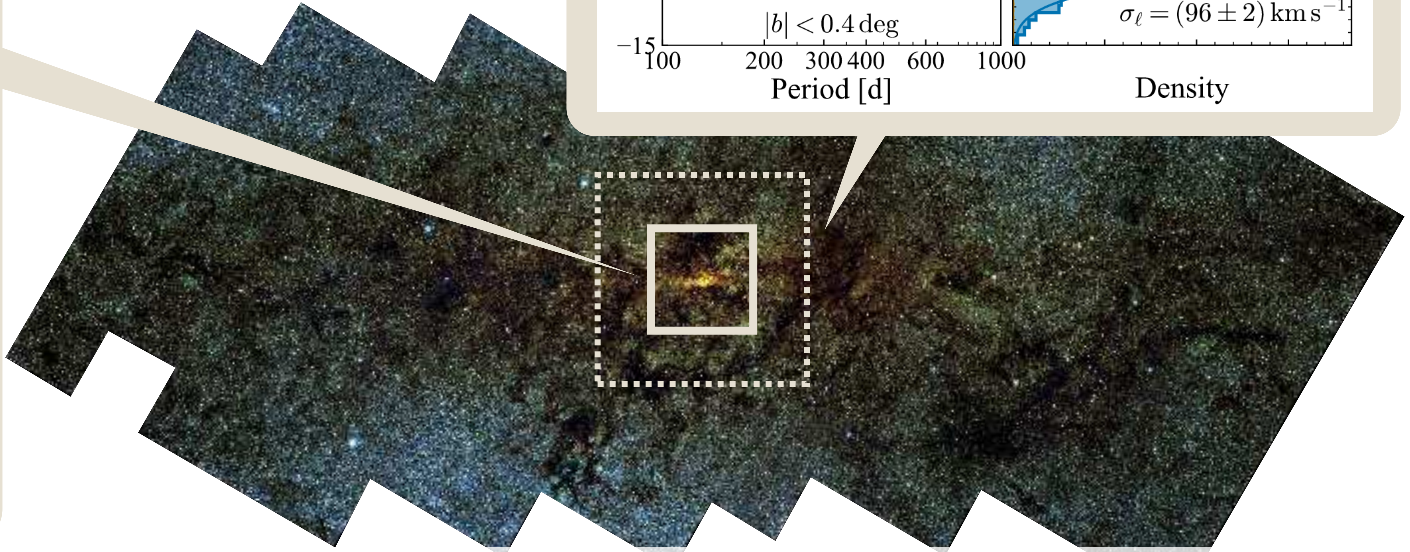

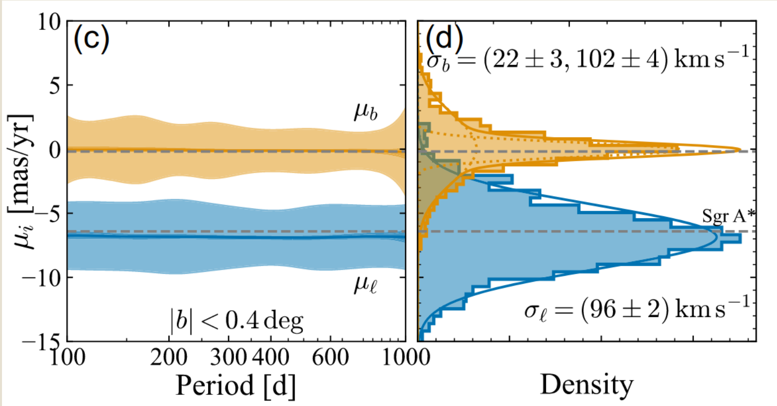

SIRIUS survey (Nishiyama+, 2006), Miras in NSD (Sanders+, 2024)

Precise Astrometry

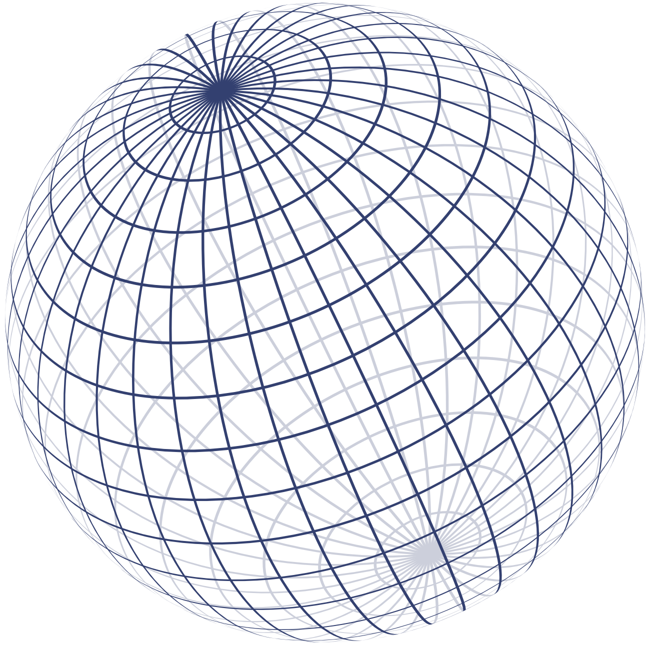

Global & Absolute

Hipparcos & Gaia

≫ size of FoV

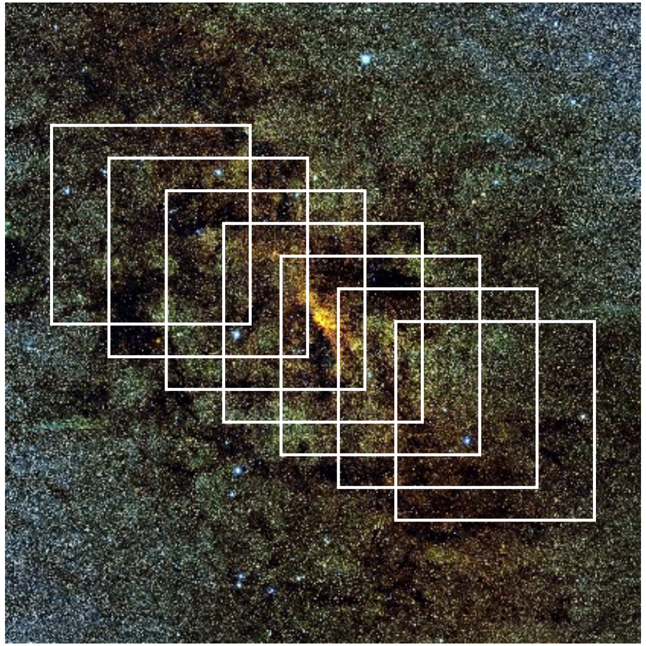

Wide-area & Relative

UCAC4, VIRAC, gVIRAC, etc.

~ size of FoV

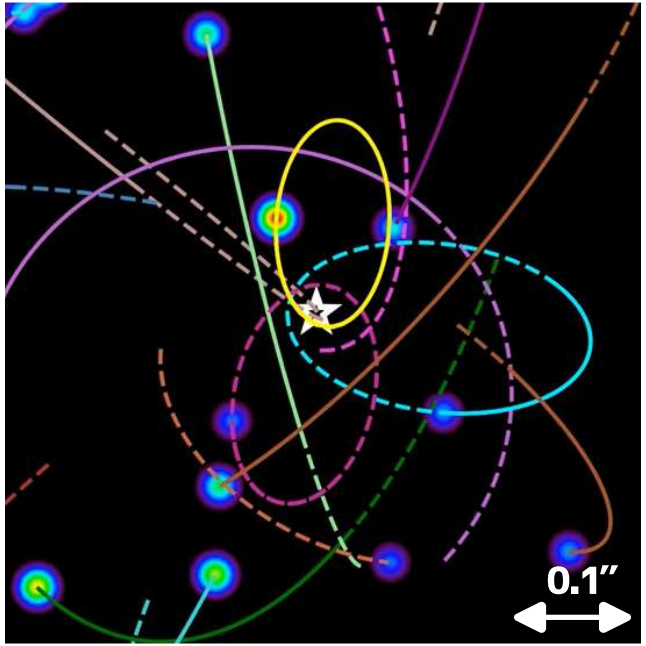

Local & Relative

Keck, HST, Theia, TOLIMAN, etc.

SIRIUS (Nishiyama+, 2006); Keck/UCLA Galactic Center Group

Precise Astrometry

Advanced data analysis
- Self-calibration
- Global self-consistent solution

≫ size of FoV

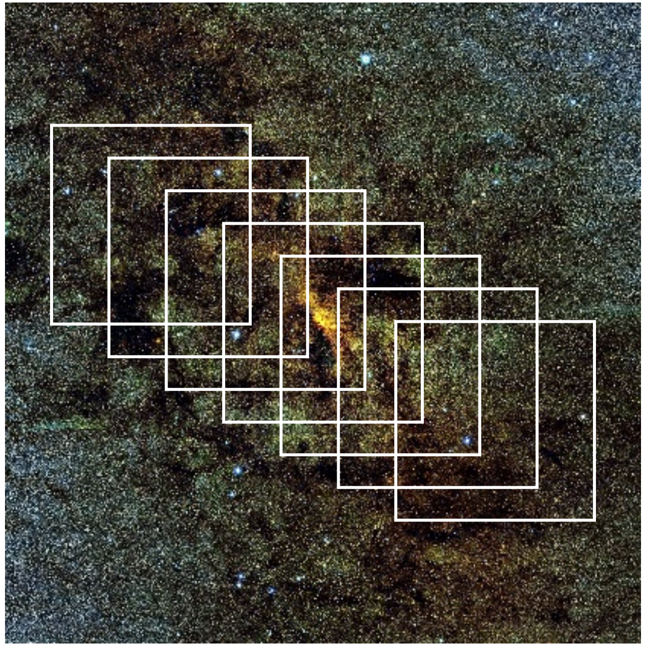

~ size of FoV

New technology
- Focal plane monitoring
- Phase masking

Global & Absolute

Hipparcos & Gaia

~10 μas

Wide-area & Relative

UCAC4, VIRAC, gVIRAC, etc.

~0.5 mas/yr

Local & Relative

Keck, HST, Theia, TOLIMAN, etc.

~1 μas

SIRIUS (Nishiyama+, 2006); Keck/UCLA Galactic Center Group

Plate Analysis

A self-calibration method

- Algorithm provides a self-consistent solution within a dataset.
- Observation model incorporates the telescope and instrument.
- Model parameters are tuned to reproduce the measurements.
- Image distortion is estimated using the measurements.

Anchoring with reference sources

- Relative astrometry requires anchoring points to fix the fields.

Simplifications

- Stellar motions are neglected within a sequence of exposures.
- Image distortion is regarded as consitant in a dataset.
- Scale (focal length) can be variable in this study.

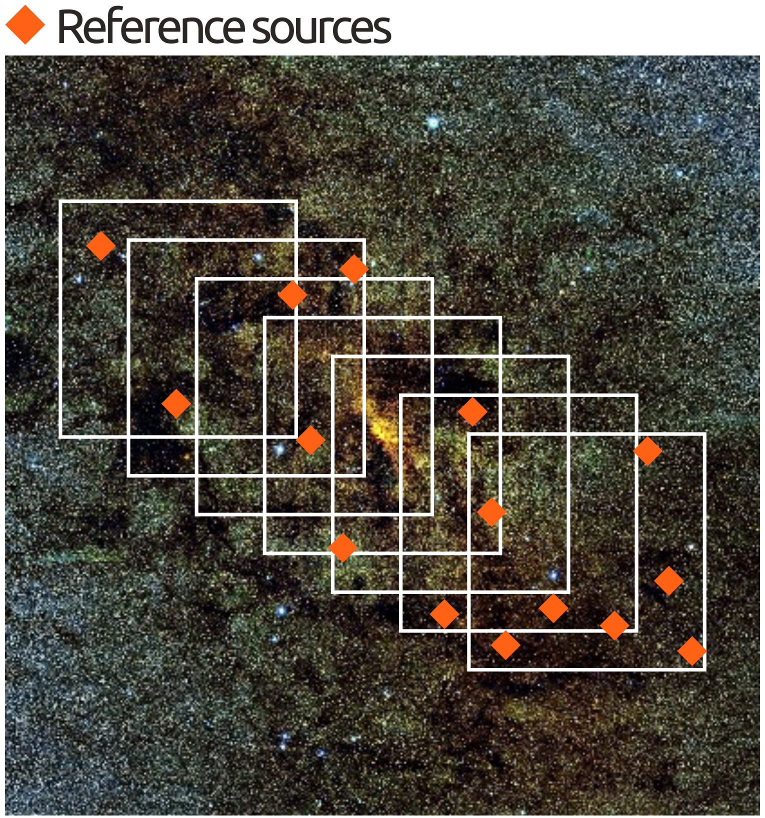

Ohsawa+, 2024, SPIE Proc., 13101-1R

Plate Analysis

Pre-established calibration data may introduce systematic errors.
Self-calibration is required to achieve an ultimate precision.

A self-calibration method

- Algorithm provides a self-consistent solution within a dataset.
- Observation model incorporates the telescope and instrument.
- Model parameters are tuned to reproduce the measurements.
- Image distortion is estimated using the measurements.

Anchoring with reference sources

- Relative astrometry requires anchoring points to fix the fields.

Simplifications

- Stellar motions are neglected within a sequence of exposures.
- Image distortion is regarded as consitant in a dataset.
- Scale (focal length) can be variable in this study.

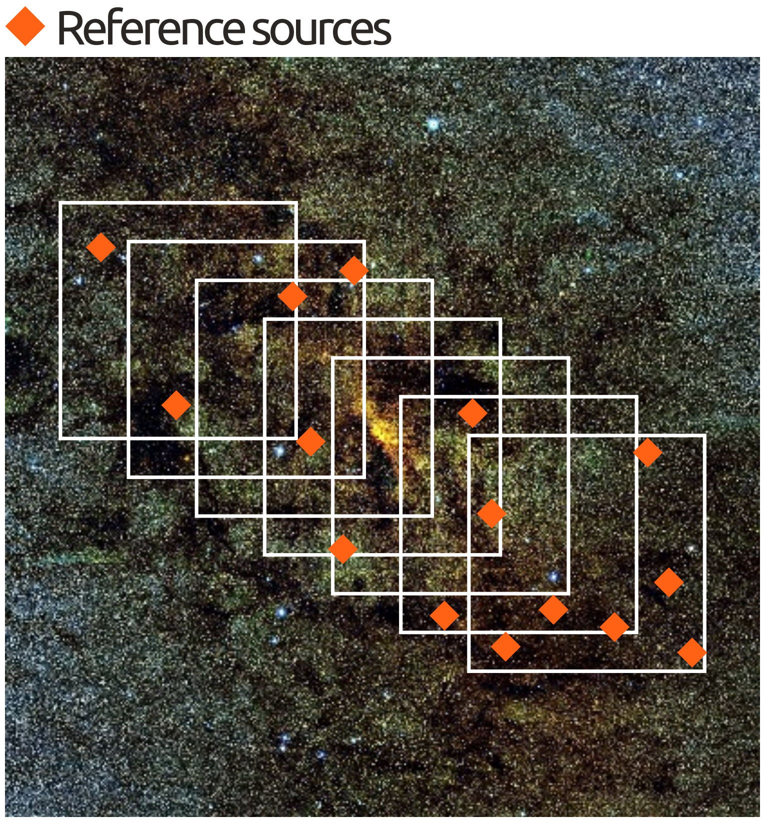

Ohsawa+, 2024, SPIE Proc., 13101-1R

Astrometric Solution

The astrometric solution is derived in the Bayesian approach.

Construct a deterministic mapping function from celestial to detector coordinates.

celestial coordinates → detector coordinates

$$(\alpha, \delta) \xrightarrow[\text{w/calibration parameters}]{} (n_x,\ n_y)$$

The posteriors of (α, δ) are defined as follows.

Posteriors of α, δ — Measurement errors — Priors

$$p(\alpha, \delta \,|\, n_x, n_y) \propto p(n_x, n_y \,|\, \alpha, \delta, \ldots)\; p(\alpha, \delta, \ldots)$$

We assume Gaussian distributions for the likelihood function

Reference information is naturally implemented as the priors

Differentiable Implementation

In general, we have to tackle with a huge model.

In this presentation
- ~ 10,000 sources
- ~ 300,000 measurements

We take advantage of the differentiable programming techniques.

celestial coordinates (α, δ) → w/calibration parameters → detector coordinates (n_x, n_y)

Using the differentiable programming library, JAX, the mapping is implemented as fully differentiable.

$$\left(\frac{\partial n_x}{\partial \alpha}, \frac{\partial n_x}{\partial \delta}, \frac{\partial n_y}{\partial \alpha}, \frac{\partial n_y}{\partial \delta}, \ldots\right)$$

The posteriors are approximated via (Stochastic) Variational Inference.

Posteriors of α, δ — Measurement errors — Priors

$$p(\alpha, \delta \,|\, n_x, n_y) \propto p(n_x, n_y \,|\, \alpha, \delta, \ldots)\, p(\alpha, \delta, \ldots)$$

$$\simeq \mathcal{N}(\alpha \,|\, \hat{\alpha}, \sigma_\alpha)\, \mathcal{N}(\delta \,|\, \hat{\delta}, \sigma_\delta)$$

Minimize the divergence between these distributions.

Poisteriors are approximated by a combination of Normal distributions.
The Bayesian inference problem is reduced to an optimazation problem.

An interesting DP application found in **P311b**

Overview of the validation process

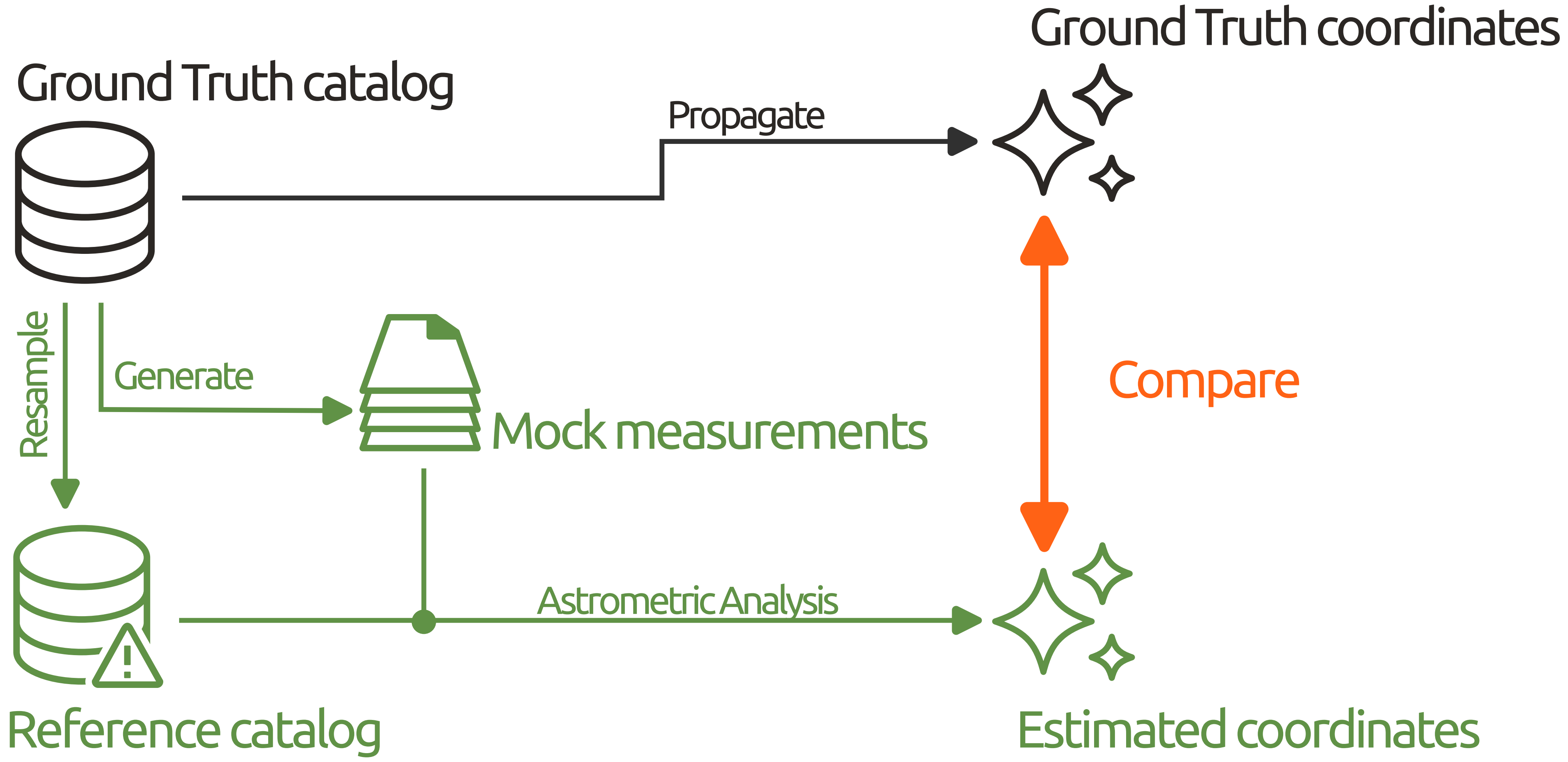

Ohsawa+, 2024, SPIE Proc., 13101-R1

JASMINE

JASMINE: Japan Astrometry Satellite Mission INfrared Exploration

An satellite mission for precise photometry and astrometry in 1.0-1.6 μm

> Measureing the proper motions and parallaxes of stars around the Galactic center.
> Image-based and small-field space astrometry mission.

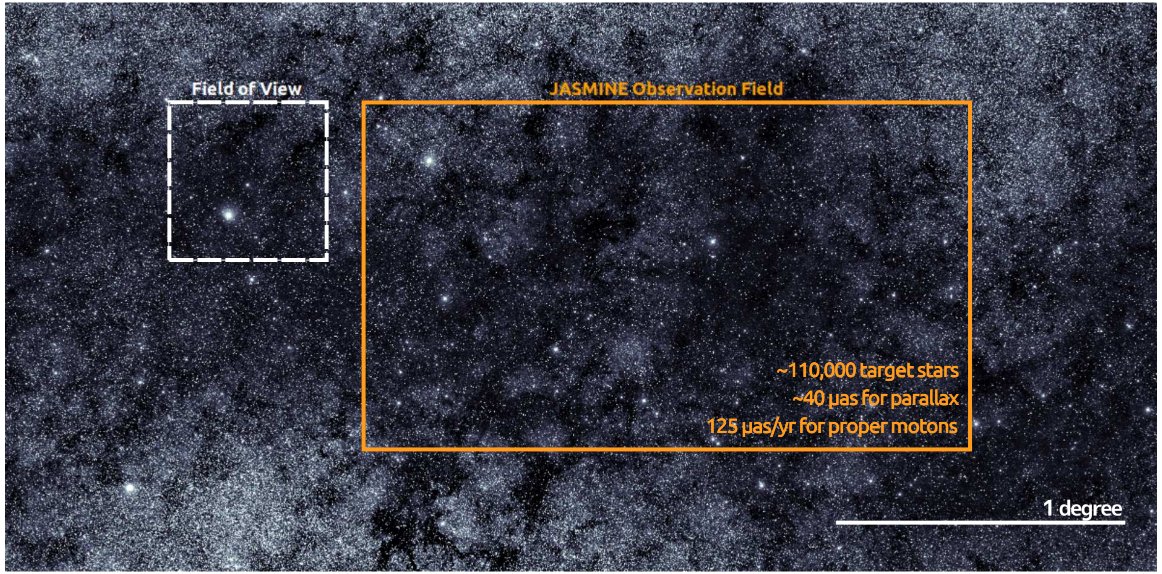

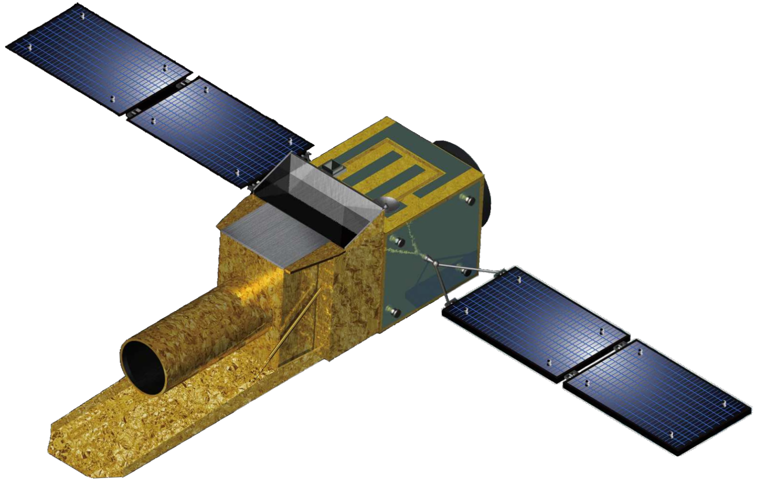

A preliminary design of the JASMINE satellite

See the SPIE proc. (Kataza+, 2024, 13092-9; Isobe+, 2024, 13092-186; Suematsu+, 2024, 13092-185)

JASMINE mini survey

	Actual mission	Mini survey
Survey field	2.1° × 1.2° region	around (l, b) = (-0.3°, 0.1°)
Epoch	>3 years	3 years
# of orbits	> 6,000	**100**
# of exposures	~ 50 per field	**24** exp × **4** fields
target stars	many bulge stars	Gaia DR3 + **artificial sources**
reference	foreground Gaia stars	~ 10,000 Gaia stars
measurement error	magnitude dependent	~ 0.01 pixel (4 mas)
relativistic aberration	Earth + satellite	Earth only
focal length	can vary every exposure	can very every exposure
image distortion	can be changed	fixed (polynomial)
stellar color	widely distributed	not included

μ=0&π=0

JASMINE mini-survey dataset is available in Zenodo (zenodo.org/records/10403895)

Results – Datasets

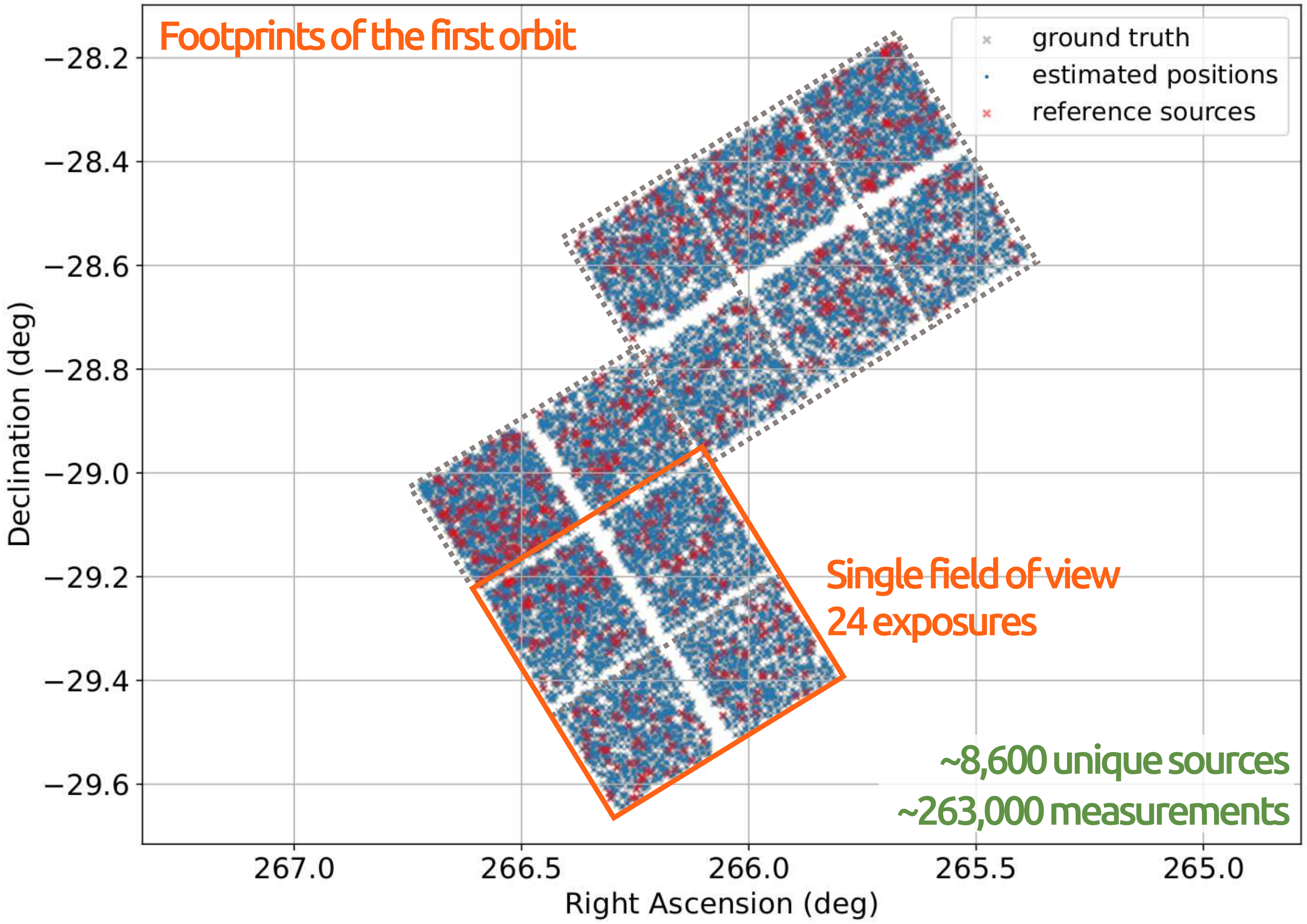

Results – Plate Analysis

The mock measurements were reproduced with an accuracy of 0.01 pixels.
The estimated coordinates wer consistent with the ground truth at a 1-mas level.

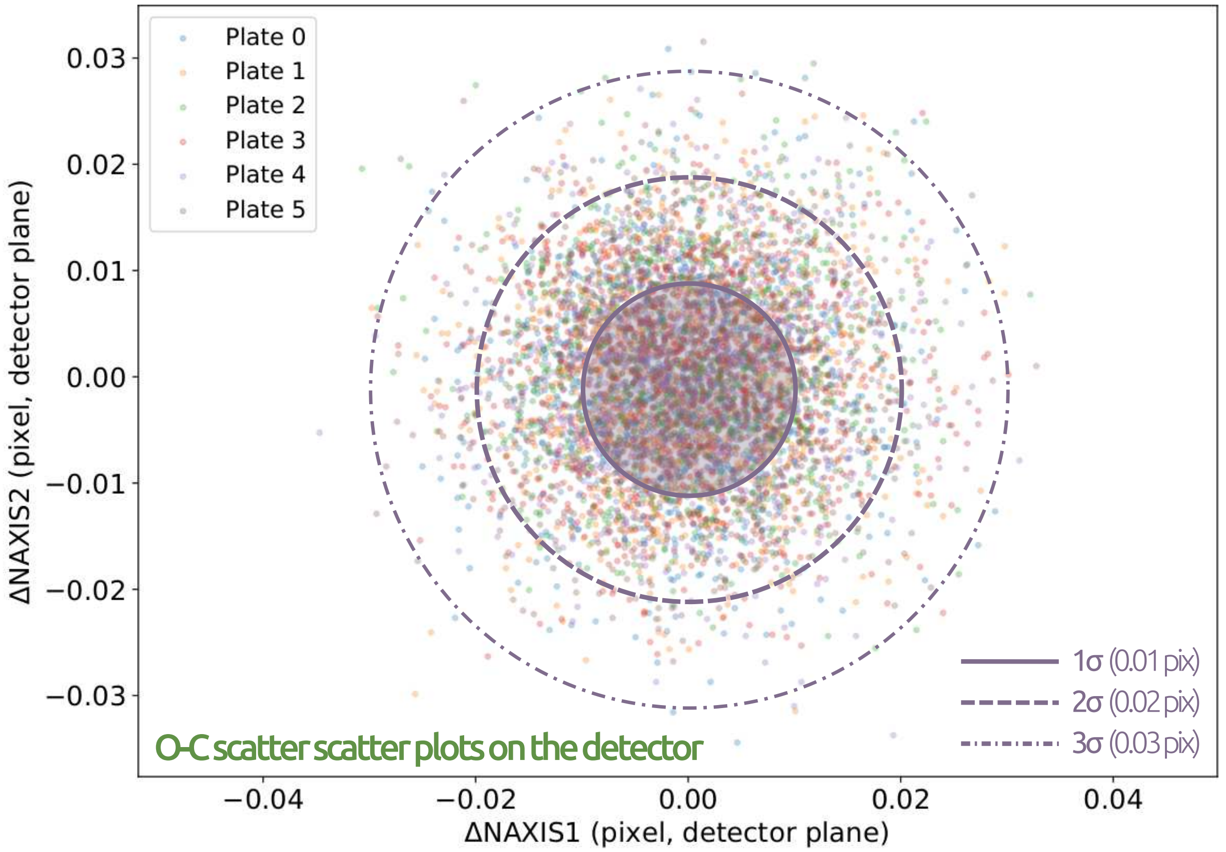

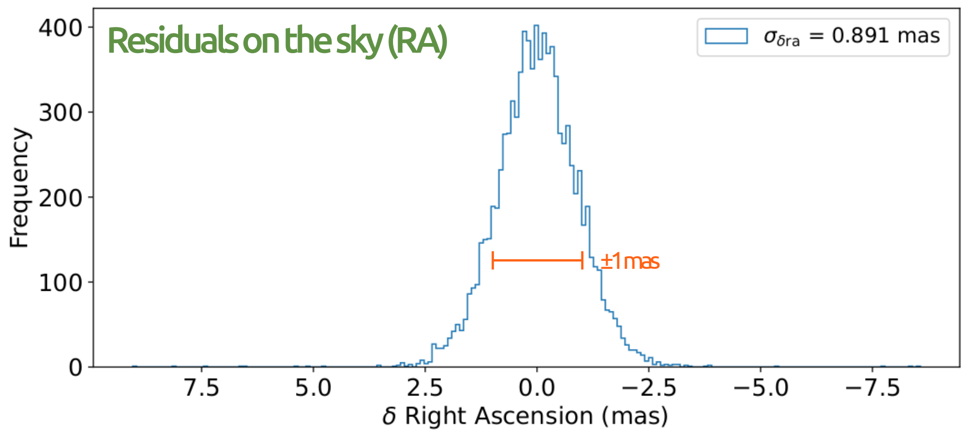

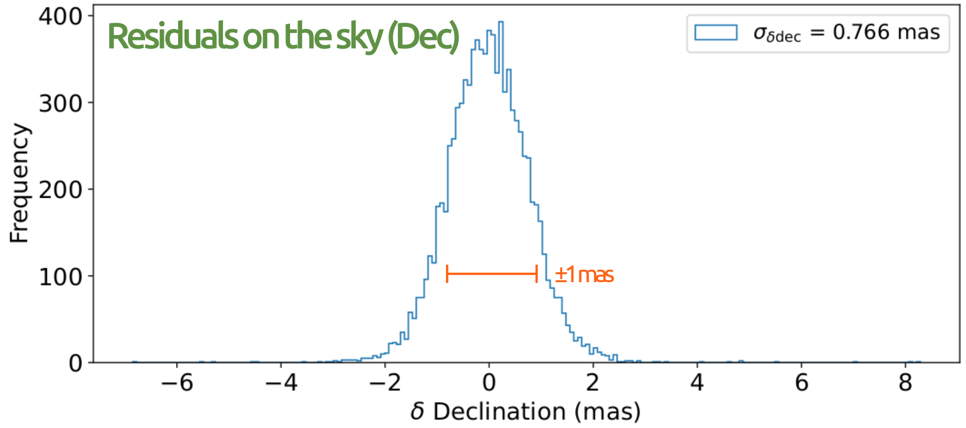

Results – Stellar Motion

Stellar motions via the 100-orbit analysis

The estimated coordinates well reproduced the proper motion + parallax motion.

Artificial sources with μ=0 & π=0 did not stay within uncertainties as expected.

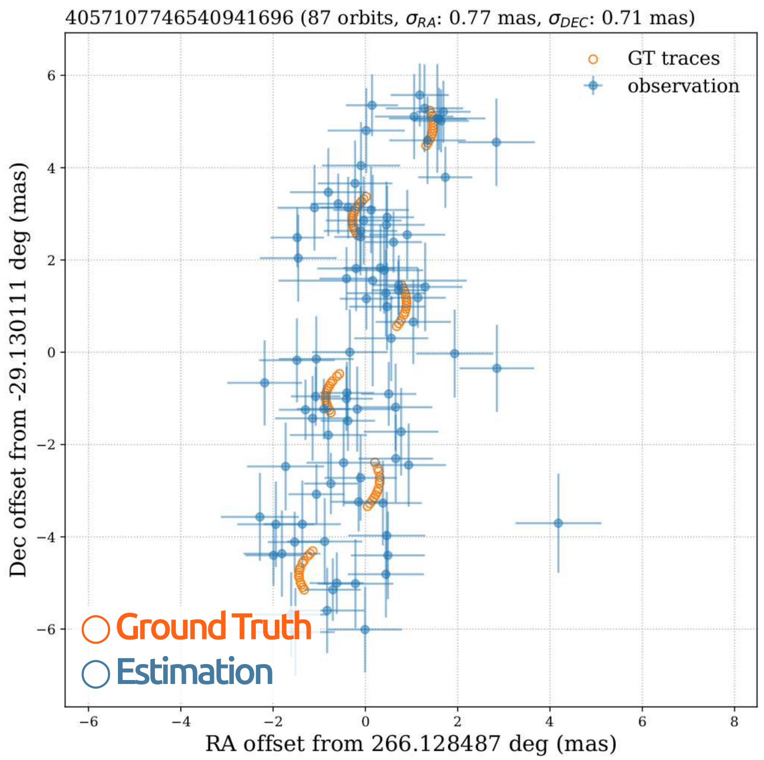

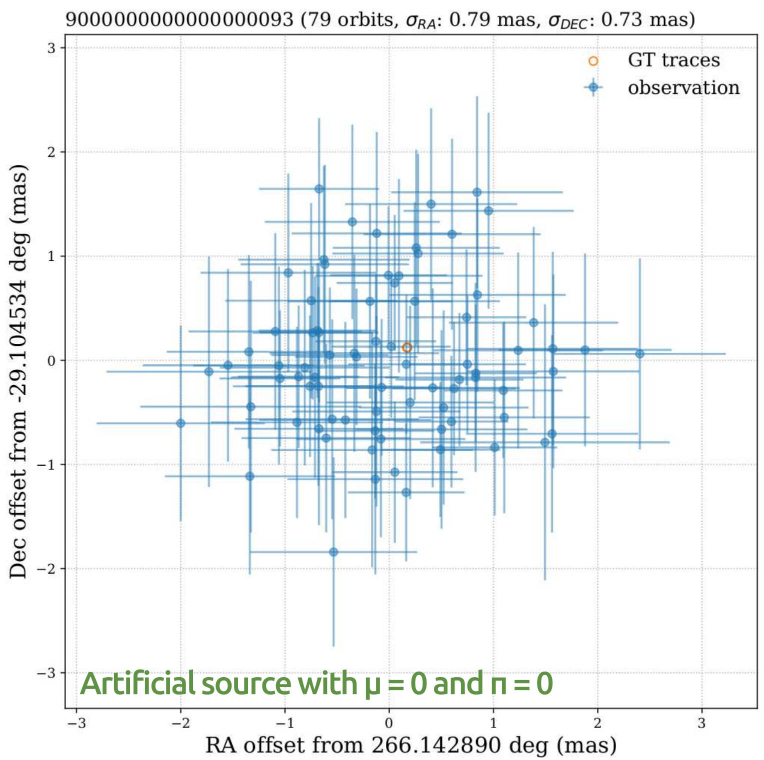

Ohsawa et al. (2024), SPIE Proc., 13101-64

Discussion

The celestial coordinates of the artificial sources were estimated by the weighted means.

The deviations from the ground truth are consistent with the measurement errors.

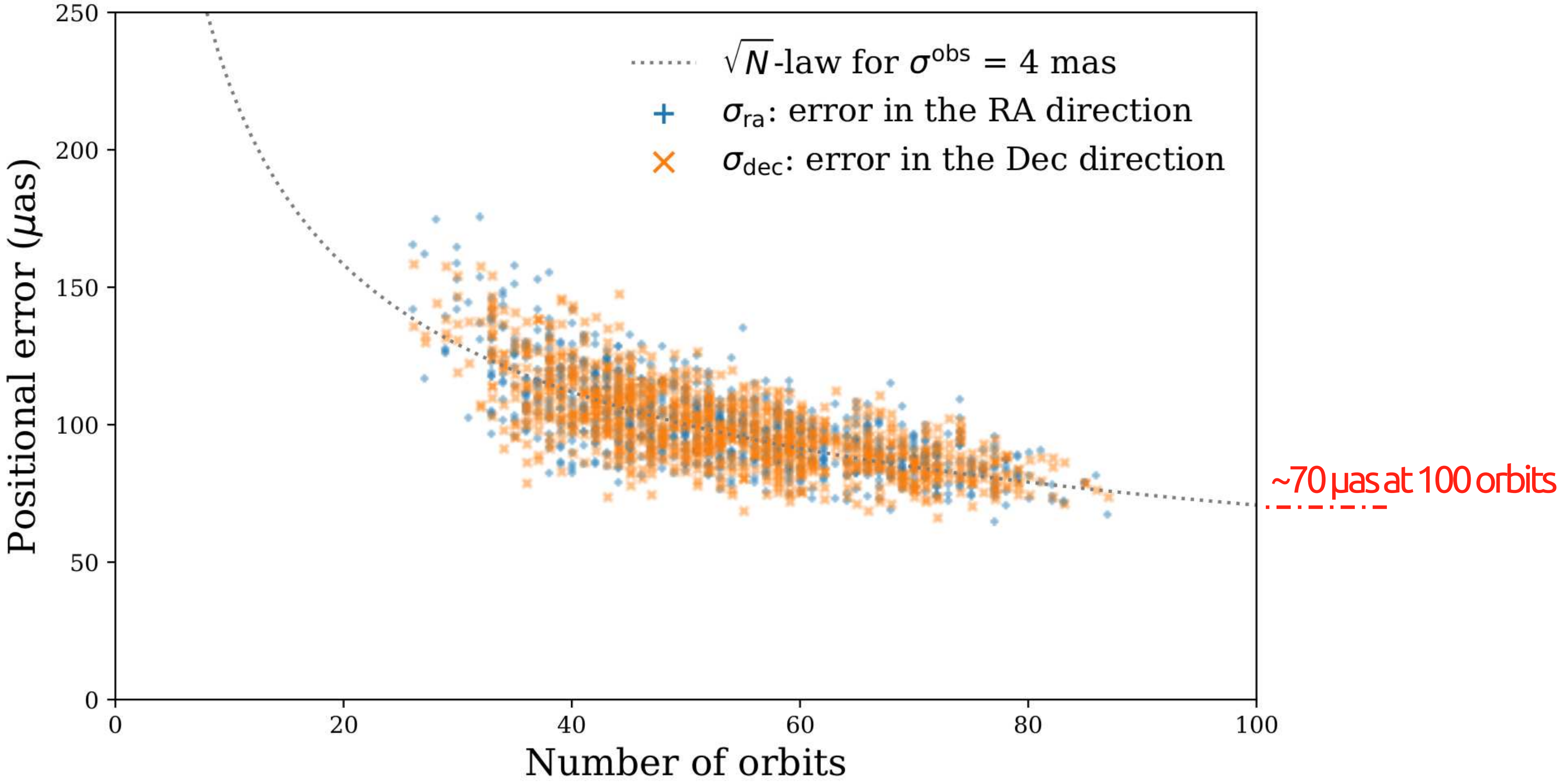

Discussion

Some reference sources were highly affected by wrong priors.

- The prior errors are mainly attributable to the propagation of the proper motion errors.
- The proper motions and parallaxes are less affected.
- The sources around such errorneous reference sources should be carefully treated.

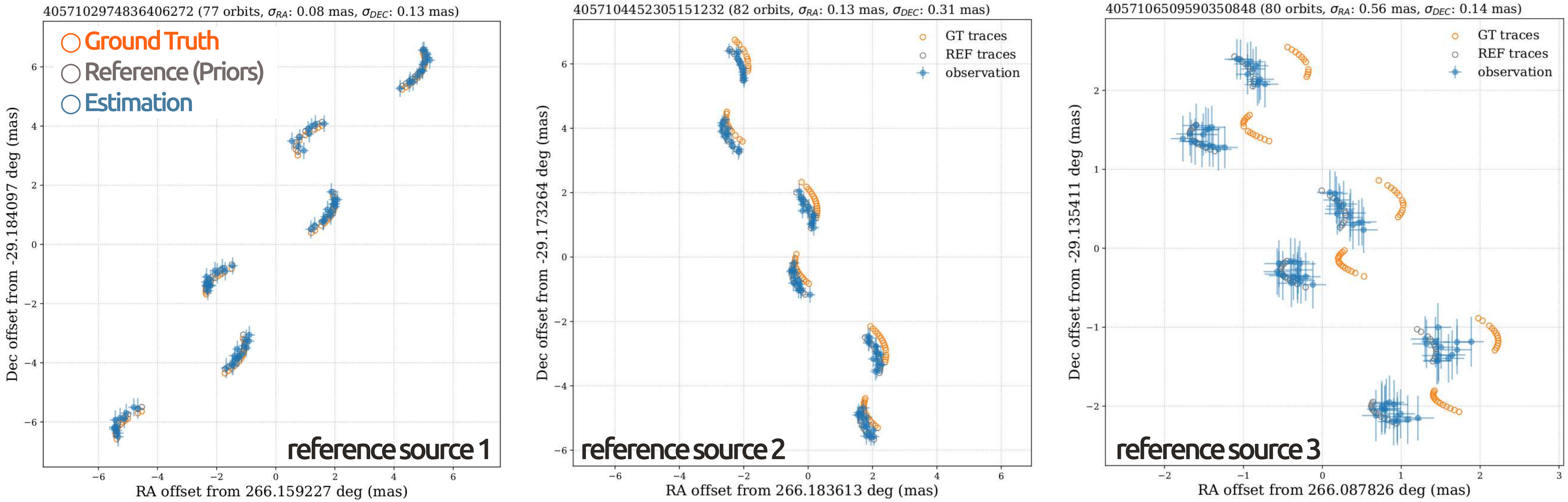

Ohsawa et al. (2024), SPIE Proc., 13101-1R

Conclusion

We developed the Plate Analysis algorithm for wide-area & relative astrometry.

Plate Analysis is based on the following assumptions.

- The apparent motions of sources are negligible within a dataset.
- The image distortion pattern is consistent within a dataset.

We developed software to obtain astrometric solutions for the Plate Analysis.

- The observation model is implemented with JAX and differentiable.
- Parameters are optimized with SVI, accelerated with JAX & numpyro.

The software successfuly provided a reasonable solution in a validation test.

Possible future update

- Loosen the assumption of the Plate Analysis to the global solution.
- Adopt more flexible distributions in the Stochastic Variational Inference.

Basic observation sequence

The satellite is in the sun-synchronous orbit on the day-night boundary (P ~ 100 min).

The telescope is pointed toward the target for the half of the satellite orbit.

The satellite attitude is controlled to stabilize the temperature for the other half.

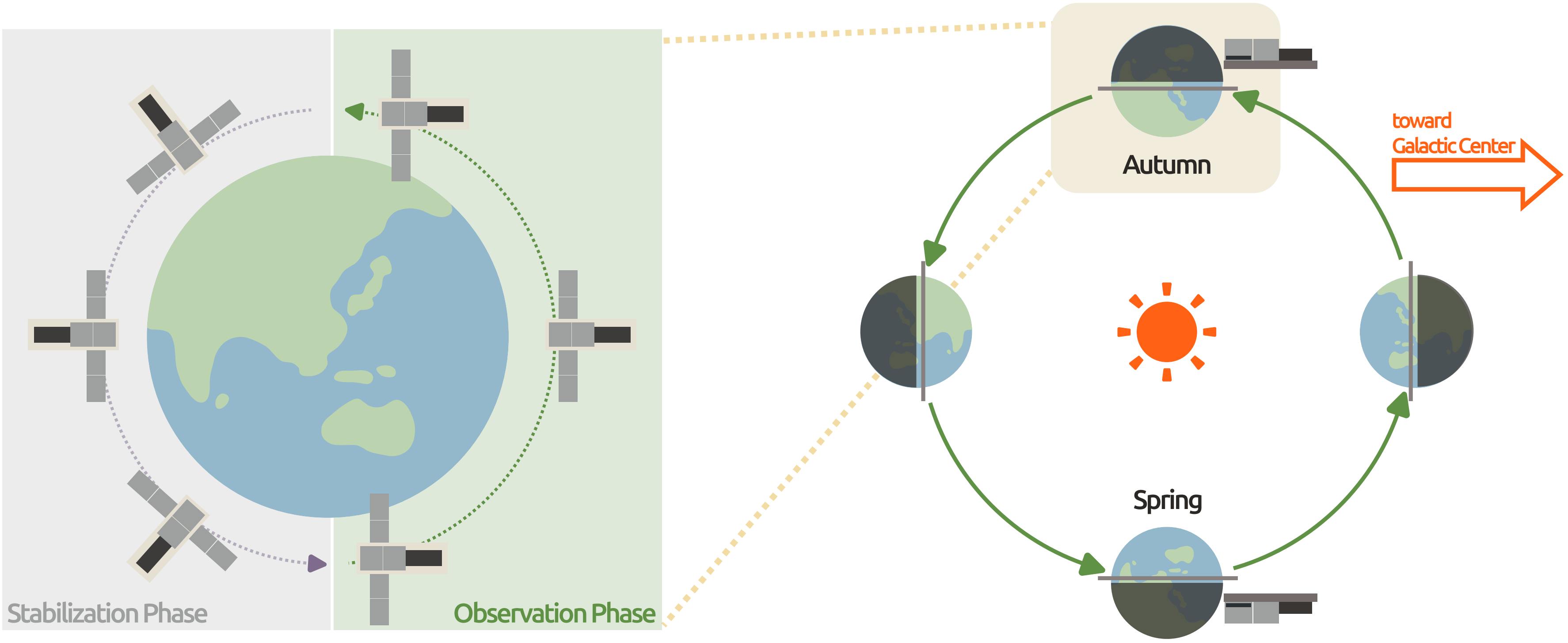

Kataza et al. (2024) SPIE Proc.,13092-9

Implementation

Group	Parameter	Symbol	Description
Source Parameters	`ra`	$\alpha_i^{\rm src}$	right ascension of the source i
	`sig_ra`	$\sigma_{\alpha,i}^{\rm src}$	uncertainty of the right ascension of the source i
	`dec`	$\delta_i^{\rm src}$	declination of the source i
	`sig_dec`	$\sigma_{\delta,i}^{\rm src}$	uncertainty of the declination of the source i
Telescope Parameters	`ra_tel`	$\alpha_m^{\rm tel}$	right ascension of the telescope direction at the exposure m
	`dec_tel`	$\delta_m^{\rm tel}$	declination of the telescope direction at the exposure m
	`theta_tel`	$\theta_m^{\rm tel}$	position angle of the telescope pointing at the exposure m
	`foc_tel_x`	$F_{X,m}$	focal plane scale along the X axis at the exposure m
	`foc_tel_y`	$F_{Y,m}$	focal plane scale along the Y axis at the exposure m
Distortion Parameters	`A_kl`	$A_{k,l}$	focal plane distortion coefficients for the X axis
	`B_kl`	$B_{k,l}$	focal plane distortion coefficients for the Y axis
Detector Parameters	`det_x`	$x_n^{\rm det}$	focal plane X coordinate of the detector n
	`det_y`	$y_n^{\rm det}$	focal plane Y coordinate of the detector n
	`det_t`	$\theta_n^{\rm det}$	focal plane rotation angle of the detector n
	`det_sx`	$\delta_{x,n}^{\rm det}$	focal plane x pixel scale of the detector n
	`det_sy`	$\delta_{y,n}^{\rm det}$	focal plane y pixel scale of the detector n

Priors

Source Parameters	ra	$\mathcal{N}(\hat{\alpha}_i^{\mathrm{p}}, \hat{\sigma}_{\alpha,i}^{\mathrm{p}})$	$\hat{\alpha}_i^{\mathrm{p}}$ and $\hat{\sigma}_{\alpha,i}^{\mathrm{p}}$ are obtained from the reference catalog
	dec	$\mathcal{N}(\hat{\delta}_i^{\mathrm{p}}, \hat{\sigma}_{\delta,i}^{\mathrm{p}})$	$\hat{\delta}_i^{\mathrm{p}}$ and $\hat{\sigma}_{\delta,i}^{\mathrm{p}}$ are obtained from the reference catalog
Telescope Parameters	ra_tel	$\mathcal{N}(\hat{\alpha}_m^{\mathrm{tel}}, \hat{\sigma}_{\alpha,m}^{\mathrm{tel}})$	$\hat{\alpha}_{i,m}^{\mathrm{tel}}$ is obtained from the environment table; $\hat{\sigma}_{\alpha,m}^{\mathrm{tel}}$ is set to 1°
	dec_tel	$\mathcal{N}(\hat{\delta}_m^{\mathrm{tel}}, \hat{\sigma}_{\delta,m}^{\mathrm{tel}})$	$\hat{\delta}_{i,m}^{\mathrm{tel}}$ is obtained from the environment table; $\hat{\sigma}_{\delta,i,m}$ is set to 1°
	theta_tel	Uniform distribution over $(-180^\circ, 180^\circ)$	
	foc_tel_x	Gamma distribution with the mean of $\hat{F}_{X,m}$ and the variance of 100.0	
	foc_tel_y	Gamma distribution with the mean of $\hat{F}_{Y,m}$ and the variance of 100.0	
Distortion Parameters	A_kl	$\mathcal{N}(\hat{A}_{k,l}, \hat{\sigma}_{k,l}^{A})$	$\hat{A}_{k,l} = 0$ and $\hat{\sigma}_{k,l}^{A} = 1.0$
	B_kl	$\mathcal{N}(\hat{B}_{k,l}, \hat{\sigma}_{k,l}^{B})$;	$\hat{B}_{k,l} = 0$ and $\hat{\sigma}_{k,l}^{B} = 1.0$
Detector Parameters	det_x	$\mathcal{N}(\hat{x}_n^{\mathrm{det}}, \sigma_{x,n}^{\mathrm{det}})$	$\hat{x}_n^{\mathrm{det}}$ is fixed to a rough estimate; $\sigma_{x,n}^{\mathrm{det}}$ is set to 100.0 µm
	det_y	$\mathcal{N}(\hat{y}_n^{\mathrm{det}}, \sigma_{y,n}^{\mathrm{det}})$	$\hat{y}_n^{\mathrm{det}}$ is fixed to a rough estimate; $\sigma_{y,n}^{\mathrm{det}}$ is set to 100.0 µm
	det_t	$\mathcal{N}(\hat{\theta}_n^{\mathrm{det}}, \sigma_{\theta,n}^{\mathrm{det}})$	$\hat{\theta}_n^{\mathrm{det}}$ is fixed to a rough estimate; $\sigma_{\theta,n}^{\mathrm{det}}$ is set to 0.1°
	det_sx	$\mathcal{N}(\hat{\delta}_{x,n}^{\mathrm{det}}, \sigma_{\delta_x,n}^{\mathrm{det}})$	$\hat{\delta}_{x,n}^{\mathrm{det}}$ is fixed to a rough estimate; $\sigma_{\delta_x,n}^{\mathrm{det}}$ is set to $0.01\,\hat{\delta}_{x,n}^{\mathrm{det}}$
	det_sy	$\mathcal{N}(\hat{\delta}_{y,n}^{\mathrm{det}}, \sigma_{\delta_y,n}^{\mathrm{det}})$	$\hat{\delta}_{y,n}^{\mathrm{det}}$ is fixed to a rough estimate; $\sigma_{\delta_y,n}^{\mathrm{det}}$ is set to $0.01\,\hat{\delta}_{y,n}^{\mathrm{det}}$

Optimization

The models are optimized using the ADAM optimizer.

$\alpha = 10^{-3}, 10^{-4}, \ldots, 10^{-10}$

The parameters are iteratively updated with decreasing learning rates.

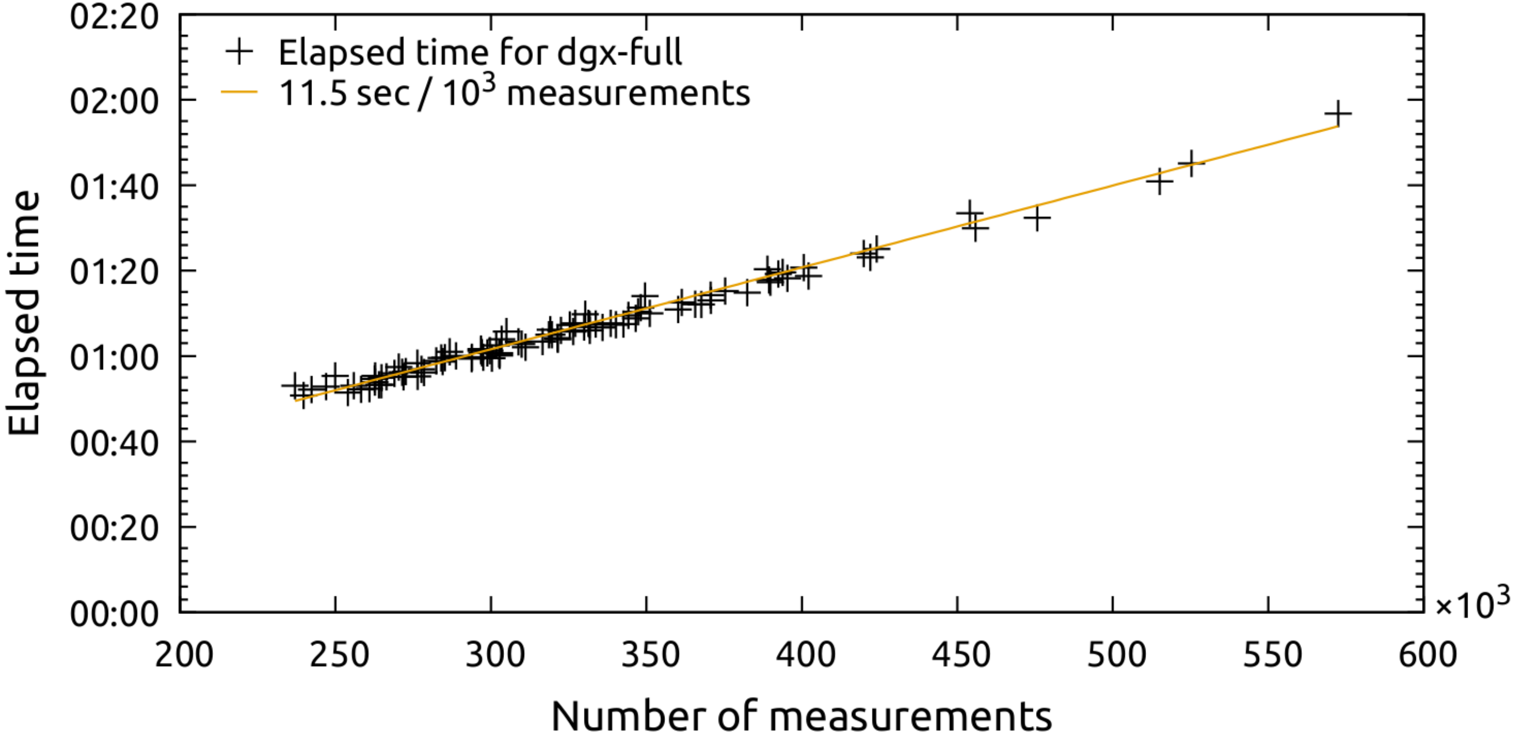

We used the GPU cluster at CfCA/NAOJ (dgx-full). Each job was parallelly executed and accelerated by a single GPU (A100, 40 GB).

JAX (Bradbury+, 2018); numpyro (Phan+, 2019)

Mission Concepts of JASMINE

The key features for the mission success:

- Optics made of extremely low-thermal-expansion materials (CTE < 10^{-8}/K).
- Sophisticated thermal design and control to achieve an effectively large thermal inertia.
- Sharp PSFs (SR > 0.9) over the entire field of view.
- Foreground sources as achors to fix and align the coordinate frame to the ICRS.
- Estimating the image distortion patterns using partially overlapped images.

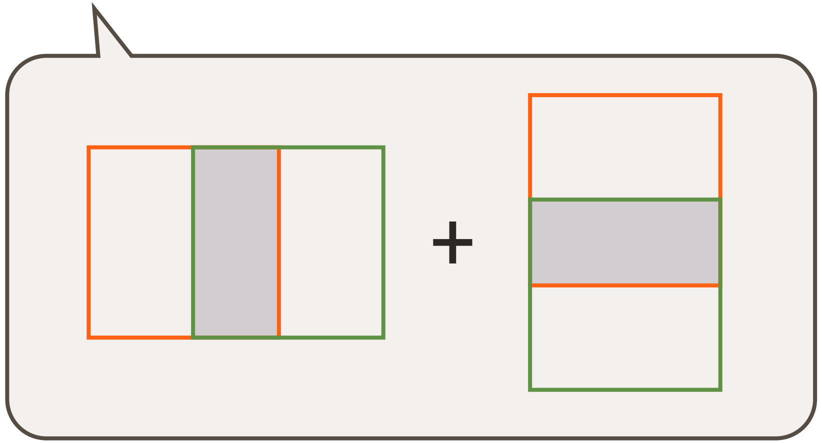

See Kataza+ (13092-9), Isobe+ (13092-186), and Suematsu+ (13092-185) in SPIE 2024